Redirected Walking with IRS-assisted Beamforming

Keh-Yeun Liao[‡], Chiao-Wen Lin[†], De-Nian Yang[♯], and Wanjiun Liao[†]
[‡]Graduate Institute of Communication Engineering, National Taiwan University, Taiwan
[†]Department of Electrical Engineering, National Taiwan University, Taiwan
[♯]Institute of Information Science, Academia Sinica, Taiwan
E-mail: {r08942125,d09921012}@ntu.edu.tw, dnyang@iis.sinica.edu.tw, and wjliao@ntu.edu.tw

ICC 2022 - IEEE International Conference on Communications | 978-1-5386-8347-7/22/$31.00 ©2022 IEEE | DOI: 10.1109/ICC45855.2022.9838715

***Abstract*—Remote working and virtual socializing are becoming the norm. This trend evokes the growth of virtual reality (VR). Users can explore virtual environments (VEs) with the most intuitive approach: walking. In contrast to traditional static VR experience, redirected walking (RW) enables users to walk in VEs larger than the physical space. Recent RW works aim to deliver an obstacle-free VR experience. However, they ignore the user's cybersickness and received signal strength, which degrades the VR experience. In this paper, we investigate Path Planning with Cybersickness and IRS Control (PPCIC) in an indoor RW system with cybersickness and IRS control. We proposed an algorithm with Cybersickness Indicator (CI) and SINR Indicator (SI) to evaluate the cybersickness and received signal strength of each path. Simulation results show that our algorithm outperforms the baselines regarding the total cost, cybersickness, and received signal strength.**

I. Introduction

Expedited by Covid-19 pandemic, the world has been transformed into remote collaboration. Remote working and virtual socializing are becoming the norm.[1] This trend evokes the concept of Metaverse[2] and accelerates the growth of virtual reality (VR). Exploring VR with joysticks is considered obsolete because it severely undermine the user immersion [1]. In contrast, users wearing VR head-mounted displays (HMDs) can explore virtual environments (VEs) with the most intuitive approach: walking. For example, Google Earth VR[3] allows users to navigate through VEs by walking. However, users cannot walk freely in physical spaces since they might collide with obstacles [2]. To allow users to explore VEs regardless of the physical space and device requirements, redirected walking (RW) is proposed to guide users wearing HMDs away from physical obstacles and boundaries by subtly adjusting the mapping (gain) between the user's actual movement (translation and rotation) and the movement in VE [3]–[5].[4] It has been demonstrated that the user immersion only deteriorates slightly when the differences are within certain thresholds [5], [6]. Recent RW works focus on finding the thresholds of redirection techniques and developing real-time RW systems [4], [7], [8]. Nevertheless, these works did not consider the wireless channel quality of users towards 6G. Finding a path that avoids obstacles while maintaining wireless channel quality is critical for RW systems to improve the user immersion.

To enhance the channel quality of areas where line-of-sight (LOS) signals are blocked, intelligent reflecting surface (IRS) has been demonstrated as a promising solution. IRS consists of a massive number of signal reflecting passive elements on a planar surface. With IRS-assisted beamforming, the desired signals can be reflected by adjusting the phase shift [9], [10], allowing RW systems to enhance users' channel quality along their path. Zhang *et al.* [11] used the pilot symbols to track the user's location and optimize the IRS phase shifts based on it. Mu *et al.* [12] created a channel power gain map and then conducted IRS and robot path planning based on it. However, the above research did not explore RW in VR with IRS.

Cybersickness is similar to motion sickness, and its symptoms include headache, nausea, etc [13]. It mainly occurs due to the differences between the user's actual motion and the motion expected by the user's eyes. Several factors causes cybersickness: 1) **RW gains**. Redirection techniques with high gains increase the differences between the real world and VE. Cybersickness aggravates due to the sensory conflict [14]. 2) **Magnitude of optical flow**. Optical flow shows the distribution of brightness change and motion velocity between two frames. VR scenes with a large amount of optical flow provoke cybersickness because the visual information within aggravates the mismatch between the real world and VE [15]. 3) **Task duration**. Longer VR exposure duration incurs more cybersickness since cybersickness accumulates over time [16]. To alleviate cybersickness, field of view (FoV) shrinking [17], [18] and depth of field (DoF) simulation [19], [20] have been proposed as two effective solutions. FoV shrinking reduces the size of the viewport by masking its outer part. Small FoV induces less cybersickness due to the less amount of visual information sent to users. DoF simulation blurs the out-of-focus objects in the VE. It reduces the visual stimulus to mitigate cybersickness. However, these works only verified the effect of the alleviation techniques but did not consider the trade-off between cybersickness and the gains of redirection techniques (to avoid hitting obstacles).

In this paper, we explore Path Planning with Cybersickness and IRS Control (PPCIC) in an indoor IRS-assisted RW system. PPCIC is designed specially for VR touring[5] rather than VR games in which users have more random behaviors. Unlike previous research of IRS path planning ignoring the impact of cybersickness and RW in VR, PPCIC takes cybersickness accumulation and RW gains into account when choosing the

[1]Forbes: https://reurl.cc/83MNYj
[2]Facebook: https://reurl.cc/V5W0Z5, NVIDIA: https://reurl.cc/1oOXLW
[3]Google Earth VR: https://arvr.google.com/earth/
[4]Several RW demo videos can be found at https://reurl.cc/XlmZ1M, https://reurl.cc/xE6pnN, and https://reurl.cc/jgvQLL
[5]VeeR: https://veer.tv/, Wander: https://reurl.cc/ARXvZE

user's path and timing of IRS adjustments. The problem is challenging due to the following new research issues. 1) **Trade-off between channel quality and cybersickness**. When obstacles stand between the user and a region with better channel quality, the user requires a path with higher RW gain to reach the region. However, if the VR contents contain a large amount of optical flow, the RW system needs to prioritize cybersickness alleviation by choosing a path with less gain. Consequently, the user may not pass through the region with good channel quality. Therefore, the path planning becomes much more complicated to simultaneously control cybersickness and maintain channel quality. 2) **Joint consideration of cybersickness accumulation and IRS adjustment**. As the user keeps enjoying VR, cybersickness aggravates over time since it accumulates. However, activating FoV shrinking and DoF simulation for a long period of time dramatically decreases the user immersion [16]. Similarly, continuously enhancing the channel quality of regions that require low RW gains to reach (but have bad channel quality) damages the overall channel quality. Therefore, finding the proper timing for FoV shrinking, DoF simulation, and IRS adjustment is critical for improving user immersion and channel quality.

To address the above issues, given the maps of physical space and VE, the user's starting position and destination, the channel power gain map, and the exhaustive search time, PPCIC carefully 1) selects the user's path with its RW gains, 2) adjusts the IRS phase shift array, and 3) tailors the user's viewport size and activating of DoF simulation. The goal is to minimize the cybersickness accumulation and the penalty of having insufficient signal-to-interference-plus-noise ratio (SINR) under the 1) obstacle avoidance and 2) IRS exhaustive search constraints (detailed in Section III). We proposed a new algorithm, named IRS-assisted RW with Cybersickness Alleviation algorithm (IRWCA) to find the optimal solution. IRWCA first executes *Redirected Walking Graph Construction* (RWGC) to construct a RW graph to sketch the correlations between the user, the physical space, and the VE under the obstacle avoidance constraint. In *Cybersickness Alleviation and Path Selection* (CAPS), IRWCA first calculates the cost of each node without adjusting IRS. Then, it introduces Cybersickness Indicator (CI) to evaluate the cybersickness induced by each path segment regarding the effects of RW gains, optical flow and cybersickness alleviation. In *IRS Phase-Shift Array Control* (IPAC), IRWCA selects the path that minimizes the cost function by examining the possible IRS phase shift under the IRS exhaustive search constraint. Moreover, IRWCA introduces SINR Indicator (SI) to evaluate the ratio of SINR that can be enhanced by adjusting the IRS phase shift array.

The rest of this paper is organized as follows. Section II introduces the RW system and Section III formulates PPCIC. In Section IV, our algorithm IRWCA is presented. The simulation results are summarized in Section V. Finally, we conclude this paper in Section VI.

II. System Model

Due to the space constraint, the notation table is provided in [21]. Following [22], we model obstacles in the physical space as polygons and consider their corners as nodes. The user's location in physical space is also included as a node. With these nodes, we build an unobstructed road map for path planning [23]. We place the IRS in the physical space according to [24]. The user's **physical position** at state t is defined as $s_t^{\mathrm{p}} = (l_t^{\mathrm{p}}, \theta_t^{\mathrm{p}})$, which includes the user's location l_t^{p} and heading orientation θ_t^{p} in the physical space. On the other hand, the **virtual position** $s_t^{\mathrm{v}} = (l_t^{\mathrm{v}}, \theta_t^{\mathrm{v}})$ includes the user's location l_t^{v} and heading orientation θ_t^{v} in the VE. A typical RW system includes two redirection techniques. Translation gain TO is to slightly re-scale the walking speed in VE, and rotation gain RO is to slightly re-orient the user to the target direction [3], [25].[6] Following [4], [6], the minimum redirect cost $MRC(s_t^{\mathrm{p}}, s_{t+1}^{\mathrm{p}}) = \frac{\beta_1 TO + \beta_2 RO}{y_{fov}(1-\gamma_{dof}\alpha_{dof})}$ evaluates the degree of the user immersion when using the best combination of TO and RO (detailed in Section IV). Note that β_1 and β_2 are tuning knobs of TO and RO.

To maintain the channel quality of the user, our system carefully examines the timing to adjust **IRS phase shift array** $\Psi = diag(\eta e^{j\phi_1}, ..., \eta e^{j\phi_N})$, where η is the reflection amplitude, ϕ_n is the phase shift of IRS element n, and N is the number of reflecting elements. Following [9], the η of each element is the same since it is sophisticated to control reflection amplitude and phase shift simultaneously. There are three baseband equivalent channels, including the signal from the AP to the user $h_u^A \in \mathbb{C}^{1\times M}$, the signal from the IRS to the user $h_u^I \in \mathbb{C}^{1\times N}$, and the signal from the AP to the IRS $h_I^A \in \mathbb{C}^{N\times M}$. At the AP, $w_u \in \mathbb{C}^{M\times 1}$ denotes the transmit precoding vector for user $u \in U$. M is the number of antennas in the AP. b_u is the information-bearing symbol of user u. The **received signal** of user u is defined as $x_t = (h_u^I \Psi h_I^A + h_u^A) \sum_{u\in U} w_u b_u + h_G$, where h_G denotes the additive Gaussian noise with zero mean [24]. According to [27], an IRS system needs to conduct beam sweeping on the whole physical space (exhaustive search) to find the optimal phase shift configuration for the user. Therefore, a time interval (exhaustive search time) is required between two phase shift adjustments for the IRS system to perform exhaustive search [28], [29]. Following [24], [30], the exhaustive search time is correlated to the number of reflecting elements because the system needs to adjust each element individually to precisely reflect the signals. We record the last state that the IRS phase shift array is adjusted with **IRS index**, which is defined as:

$$\rho_t = \begin{cases} t, & \text{if IRS adjusted at state } t \\ \rho_{t-1}, & \text{otherwise} \end{cases}, \rho_0 = -\lambda \quad (1)$$

The channel power gain of the AP (with M antennas) precoding vector is measured beforehand to build a channel quality map according to [12].

To alleviate cyberisickness, the system is equipped with two cybersickness alleviation techniques, FoV shrinking [17], [18] and DoF simulation [19], [20]. DoF simulation casts rays from the user toward the VR scene to find the focus distance and then apply the bokeh filter to create dynamic blurring effect

[6]We can combine TO and RO to achieve other redirection techniques, e.g., curvature [26].

[19]. $\alpha_{dof} \in \{0, 1\}$ shows whether DoF simulation filter is activated. γ_{dof} is the ratio of blurred images on the HMD screen produced by the DoF simulation [19], [20]. As for FoV shrinking, it slightly masks the upper and lower side of the viewport to shrink FoV size. $y_{fov} \in [0, 1]$ is the ratio of shrunken viewport size to original viewport size [17], [18].

We measure cybersickness severity by the Simulator Sickness Questionnaire (SSQ) metric, which can be calculated by the magnitude of optical flow and RW gain [6]. Following [1], [13], the **accumulated cybersickness** $Q_t = Q_{t-1} + \frac{y_{fov}(1-\gamma_{dof}\alpha_{dof})(F(s^{\mathrm{p}}_{t-1}, s^{\mathrm{p}}_t)+(\beta_1 TO+\beta_2 RO)-K}{\Omega}$ represents the quantity of accumulated cybersickness after the user enters VE. Q_{t-1} is the amount of cybersickness accumulated until the last state, and $\frac{y_{fov}(1-\gamma_{dof}\alpha_{dof})(F(s^{\mathrm{p}}_{t-1}, s^{\mathrm{p}}_t)+(\beta_1 TO+\beta_2 RO)-K}{\Omega}$ represents the amount of cybersickness induced by the current state. Note that β_1 and β_2 are tuning knobs of TO and RO. $F(s^{\mathrm{vp}}_{t-1}, s^{\mathrm{vp}}_t)$ denotes the function calculating optical flow in the current state [15]. K is the rate of cybersickness dissipation due to users adapting to the VE [13], and Ω is the user's endurance to cybersickness. The endurance is affected by age, gender, anxiety, and the familiarity with VR [13].

III. Problem Formulation

In this section, we formulate Path Planning with Cybersickness and IRS Control (PPCIC) for RW path planning, IRS phase shift array control, and cybersickness alleviation of an indoor VR navigation system. In the following, the system status consisting of the physical space and VE information at state t is defined as $s^{\mathrm{vp}}_t = \{s^{\mathrm{p}}_t, s^{\mathrm{v}}_t, \Psi, x_t, \rho_t, Q_t\}$, where $s^{\mathrm{p}}_t, s^{\mathrm{v}}_t, Q_t, \Psi, x_t$, and ρ_t denote the status of physical position, virtual position, IRS phase shift array, user received signal, IRS index, and accumulated cybersickness, respectively.

The user's 1) **physical position** s^{p}_t records the user's location and heading orientation in the physical space, and 2) **virtual position** s^{v}_t records the user's location and heading orientation in the VE. We build the unblocked RW graph and calculate the RW gains of each path segment based on the physical and virtual positions. 3) The **IRS phase shift array** Ψ records the reflection amplitude and phase shift of each IRS reflecting element. 4) The **received signal** x_t consists of the signal transmitted directly from the AP to the user, the signal from the AP to IRS then to the user, and the additive Gaussian noise at the user's receiver. It is used to calculate the SINR at each state. 5) The **IRS index** ρ_t records the last state that the IRS phase shift array is adjusted. We ensure that the IRS is available for the adjustment by examining the difference between the IRS indexes of two states. 6) The **accumulated sickness** Q_t represents the quantity of cybersickness since the user enters VE. Q_t consists of the cybersickness accumulated from the last state and the cybersickness induced by the current state. A large amount of optical flow and high RW gains aggravate cybersickness, and we can activate FoV shrinking and DoF simulation to alleviate it. However, MRC increases with the activation of FoV shrinking and DoF simulation. Higher MRC increases the chance of user noticing that the VE is manipulated, which degrades the user immersion [3].

Given the map of physical space and VE, the starting status state, destination l^{p}_d of the user, channel power gain map, and the IRS exhaustive search time. PPCIC aims to find 1) a path P for the user to reach l^{p}_d and the corresponding RW gains, 2) the timing of IRS adjustment, 3) the size of the viewport, which is configured by FoV shrinking, and 4) the activation of the DoF simulation. The objective consists of the accumulated cybersickness Q_t and the SINR penalty $PEN(l^{\mathrm{p}}_t, \rho_t)$. Following [31], the SINR penalty function $PEN(l^{\mathrm{p}}_t, \rho_t)$ represents the difference between the expected signal strength and the received one at state t,

$$PEN(l^{\mathrm{p}}_t, \rho_t) = \begin{cases} |SINR_t - J|, & \text{if } SINR_t < J \\ 0, & \text{otherwise} \end{cases} \quad (2)$$

where J represents the minimum acceptable SINR for the user [29]. Therefore, the objective is $\delta Q_t + \zeta \sum_{\forall l^{\mathrm{p}}_t \in P} PEN(l^{\mathrm{p}}_t, \rho_t)$, where δ and ζ are tuning knobs to trade-off cybersickness against channel quality.

PPCIC has the following constraints, 1) **Obstacle avoidance constraint:** In order to keep users away from the physical obstacles, the system must maintain the distance between the user and obstacles, i.e., $d_{obst}(l^{\mathrm{p}}_i) \geq D_{obst}, \forall i = 1, 2, ..., t$, where $d_{obst}(l^{\mathrm{p}}_i)$ measures the distance between the physical location l^{p}_i and obstacles, and D_{obst} is the minimum required distance between the user and obstacles. 2) **IRS exhaustive search constraint:** The IRS system sweeps the environment to find the user's location and obtain the optimal phase shift setting. Therefore, we ensure that the time interval is long enough for the next exhaustive search by examining the IRS index between two states, i.e., $\rho_i - \rho_{i-1} \geq \lambda, \forall i = 1, 2, ..., t$, where λ is the exhaustive search time.

Definition 1 (PPCIC)**.** Given the maps of physical space and VE, the user's starting state and destination l^{p}_d, the channel power gain map, and the exhaustive search time λ. PPCIC finds 1) a path P with its RW gains for the user to reach l^{p}_d, 2) the timing of IRS adjustment, 3) the size of viewport (configured by FoV shrinking), and 4) the activation of DoF simulation. The objective is to minimize the user's accumulated cybersickness and the penalty of having insufficient SINR along P, i.e., $\min(\delta Q_d + \zeta \sum_{\forall l^{\mathrm{p}}_t \in P} PEN(l^{\mathrm{p}}_t, \rho_t))$, under the 1) *obstacle avoidance* and 2) *IRS exhaustive search* constraints.

IV. Algorithm

To effectively solve PPCIC, we design algorithm IRWCA to minimize the accumulated cybersickness and SINR penalty by evaluating cybersickness indicator (CI) and SINR indicator (SI). With CI, IRWCA records the cost regarding the RW gains and optical flow for each edge in the graph without adjusting IRS phase shift array. Moreover, IRWCA introduces SI to evaluate the signal strength that can be enhanced by adjusting IRS phase shift. IRWCA adjusts IRS phase shift to the optimal direction to minimize the user's total cost (objective). IRWCA consists of three phases, 1) Redirected Walking Graph Construction (RWGC), 2) Cybersickness Alleviation and Path Selection (CAPS), and 3) IRS Phase-Shift Array

Control (IPAC). RWGC builds up the RW graph and deletes the edges that do not satisfy the obstacle avoidance constraints. CAPS exploits the unobstructed graph to calculate the cost without modifying the IRS phase shift at each node and select path segments accordingly. Last, IPAC finds the best timing to adjust IRS phase shift at each node to minimize the user's total cost. Due to the limited space, more details can be founded in [21].

A. Redirected Walking Graph Construction (RWGC)

To construct an unblocked RW graph, RWGC first models the obstacles in the physical space as polygons and consider their corners as nodes. The user's physical location is also modeled as a node. With these nodes, RWGC build a graph allowing the user to walk in an unobstructed environment starting from location O. Each node $v_i \in V$ represents a physical location. l^{p}_{dst} and l^{v}_{dst} represent the destination in physical world and VE, respectively. A directed edge (i,j) exists if the user can walk from l^{p}_i to l^{p}_j under the obstacle avoidance constraint. In RWGC, each path segment (edge) has its RW gain values to re-scale the walking speed and re-orient the user's heading direction. We first calculate μ, the ratio of the distance from O to l^{v}_{dst} to the distance from O to l^{p}_{dst}. Based on μ, we can find TO and RO values for (i,j) such that the length of $(l^{\mathrm{v}}_i, l^{\mathrm{v}}_j)$ projecting onto $\overline{Ol^{\mathrm{v}}_{dst}}$ is μ times the length of $(l^{\mathrm{p}}_i, l^{\mathrm{p}}_j)$ projecting onto $\overline{Ol^{\mathrm{p}}_{dst}}$. RWGC chooses the (TO, RO) pair that minimizes $\beta_1 TO + \beta_2 RO$ and stores the according value in (i,j) along with the cybersickness and SINR (from the channel quality map mentioned in Section II) of (i,j).

Example 1. In Fig.1, src and dst denote the source and destination, respectively. RWGC removes node 6 and its edges because it violates the obstacle avoidance constraint.

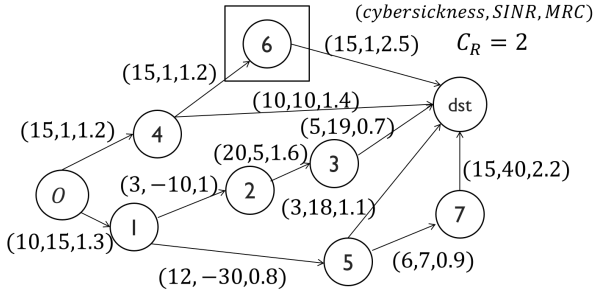

Fig. 1: Example of RWGC

B. Cybersickness Alleviation and Path Selection (CAPS)

CAPS calculates the cost of each edge without modify IRS phase shift. We introduce CI to evaluate the balance between cybersickness and RW gains. An edge with more RW gains and optical flow induces more cybersickness. When users feel dizzy, it is essential to alleviate cybersickness with FoV shrinking and DoF simulation. However, FoV shrinking and DoF simulation decrease the user immersion. Therefore, we define $CI = \frac{y_{fov}(1-\gamma_{dof}\alpha_{dof})(F(s^{\mathrm{vp}}_{t-1}, s^{\mathrm{vp}}_t)+(\beta_1 TO+\beta_2 RO)-K}{\Omega}$ to measure the cybersickness induced by each edge regarding the effect of optical flow, RW gains, FoV shrinking, and DoF simulation. To jointly minimize cybersickness accumulation and maintain channel quality, our idea is to iteratively derive the dynamic programming state of each node with the IRS configuration at each state. Let $\mathbb{E}(v_j, \rho_t, \tau)$ be the total cost when the user is on v_j at state t. We record the condition of the IRS at the current state with τ. If IRS is not available, $\tau = -1$. If IRS adjust during the current state, $\tau = 1$. If IRS is available while the system did not execute an adjustment, $\tau = 0$. For each node v_j, CAPS recursively examines the $\mathbb{E}(v_i, \rho_{t-1}, \tau), \forall v_i \in pre(j), \tau \in \{0, -1\}$, where $pre(j)$ is the set of all predecessor nodes of v_j. Then, it chooses the minimum $\mathbb{E}(v_i, \rho_{t-1}, \tau) + \delta CI + \zeta PEN(v_j, \rho_t)$ to minimize the cybersickness accumulation and SINR penalty function. Accordingly, $\mathbb{E}(v_j, \rho_t, \tau) = \min\{\mathbb{E}(v_i, \rho_{t-1}, \tau) + \delta CI + \zeta PEN(v_j, \rho_t)\}, \forall v_i \in pre(j), \forall \tau \in \{0, -1\}$.

Example 2. In Fig.2, assuming $\lambda = 3, J = 20$, $F(3, dst) = 50$, $\beta_1 = 0.25$, $\beta_2 = 0.15$, $TO = 1.6$, $RO = 2$, $K = 0.504$, $\Omega = 3.6$, $y_{fov} = 0.8$, $\gamma_{dof} = 0.1$, $\alpha_{dof} = 1$, $\delta = 0.5$, and $\zeta = 1$, we find $\mathbb{E}(v_{dst}, 0, 0)) = \mathbb{E}(v_3, \rho_3, 0)) + \delta CI + \zeta PEN(v_{dst}, 0) = 83 + 0.5 \times \frac{0.8(1-0.1\times1)(50+(0.25\times1.6+0.15\times2))-0.504}{3.6} + |19 - 20| = 89$, $\mathbb{E}(v_{dst}, 1, 0)) = 84$, $\mathbb{E}(v_{dst}, 2, -1)) = 59$, and $\mathbb{E}(v_{dst}, 3, -1)) = 74$.

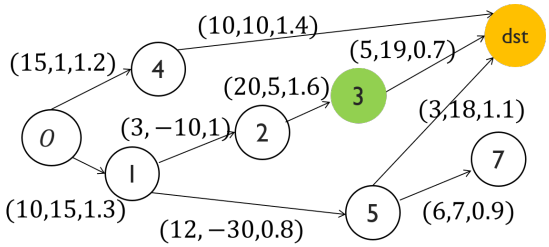

Fig. 2: Example of CAPS

C. IRS Phase-Shift Array Control (IPAC)

When the obstacles block the LOS signal in the indoor environment, it will decline the quality of user experience. Therefore, to enhance the signal strength of the user, we introduce $SI(j,t,t') = \mathrm{argmin}_{\rho_x}(PEN(v_j, \rho_x) - PEN(v_j, \rho_t)), \forall x \in [0, t']$. IPAC iteratively examine whether to adjust the IRS phase shift array at each stage. Since the IRS has a time constraint between two adjustments, IPAC check cost function for at least λ nodes away from the current node where λ is set based on the IRS exhaustive search constraint. Therefore, the cost value with IRS beam direction point to the user's location $\mathbb{E}(v_j, \rho_t, 1)) = \mathbb{E}(v_i, SI(j,t,t-\lambda), \tau)) + \delta CI + \zeta PEN(v_j, \rho_t)$, $\forall v_i \in pre(j)$ If the current node has the minimum cost function among all predecessor nodes, update the IRS index to record IRS phase shift and precoding vector on the AP toward the current location.

After repeating CAPS and IPAC with all nodes on the input graph, we can find the optimal path that minimizes the accumulated cybersickness and signal strength penalty by inducing the minimum $\delta Q_d + \zeta \sum_{\forall v_i \in P} PEN(v_i, \rho_T)$

Example 3. In IPAC, we calculate $\mathbb{E}(v_{dst}, 4, 1))$ to find the proper states to adjust IRS. Assuming $\lambda = 3$, we check $SI(dst, t, t-3)$ to obtain $\mathbb{E}(v_{dst}, 4, 1))$. $SI(dst, 4, 1) = 1$ Therefore, $\mathbb{E}(v_{dst}, 4, 1)) = \mathbb{E}(v_3, SI(dst, 4, 1), 1)) + \delta CI + \zeta PEN(v_{dst}, \rho_{dst}) = 78 + 5 + 0 = 83$. Fig. 3 shows the output

of IRWCA. The optimal path is $O \rightarrow 1 \rightarrow 5 \rightarrow dst$ and the IRS adjusts its phase shift at node 5.

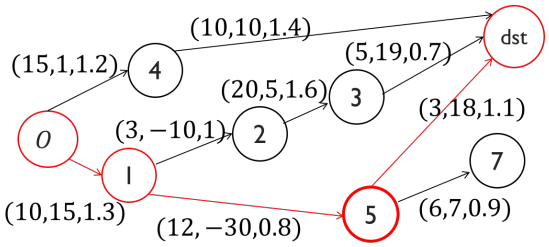

Fig. 3: The result of IRWCA

V. Simulations

A. Simulation Setup

We evaluate the performance of IRWCA with real physical space setups and IRS deployments. The indoor physical space is arranged following [32], and the number of obstacles is set to 3 accordingly. We put polygon obstacles at certain locations according to [32]. Following [9], [10], the IRS system is deployed in the indoor space. Following [33], the physical space has a fixed size of $20m \times 20m$, and a cell size of $1m \times 1m$ is used for the grid [32], [33]. The upper bounds of rotation gain and translation gain are set to 1.24 and 1.26, and the lower bounds are set to 0.67 and 0.86, respectively [4]. The MRC upper bound based on the 75% of humans detection of RW manipulations is set to $C_R = 2$ [4]. The SINR requirement is set to 50 dB in default [29] We follow [13] to set the user endurance of VR to $\Omega = 5$ and the VR adaptation K to 1. The γ_{dof} is set to 0.1 based on the result of applying DoF simulation to the rendered frames [19]. For IRS, the exhaustive search time is set to $\lambda = 3$ [9]. The η is set to 1 according to [24]. The default setting of δ and ζ are 0.5 and 1, respectively.

We compare IRWCA with three indoor path planning approaches with IRS and augment them with RW: 1) Alignment-based Redirection Control (ARC) [11], [32], 2) IRS with fixed interval and Redirected Walking (IRSRW) [11], [34], and 3) Robot Path planning (RP) [12]. ARC chooses the path with the smallest RW gains to alleviate cybersickness and adjusts the IRS phase shift at a fixed interval. IRSRW predicts the possible paths and redirects the user to avoid collisions. It sends a pilot signal to obtain the user's current location and adjust the IRS beam direction accordingly. RP builds a channel power gain map to record the channel condition at each area and minimizes the traveling time between two locations based on it. We change the following parameters: 1) the number of obstacles, 2) MRC upper bound (C_R), and 3) VR adaptation (K), and we measure the following performance metrics: 1) total cost, 2) accumulated cybersickness, 3) total SINR, 4) total MRC. Each result is averaged over 200 samples.

B. Simulation results

In Fig. (a), the total cost increases as the number of obstacles grows since the user requires redirection techniques with higher RW gain to avoid hitting obstacles, but it induces more cybersickness (in Fig. 4(b)). As the number of obstacles increases, IRWCA outperforms others since it uses

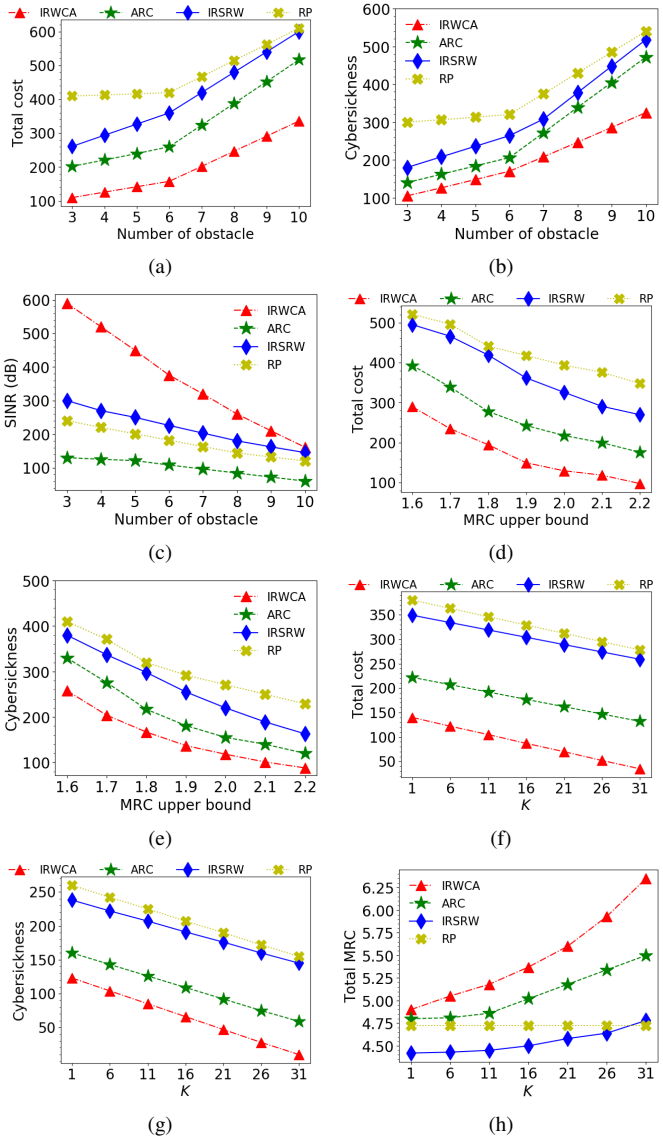

Fig. 4: Performance evaluation with different parameters.

FoV shrinking and DoF simulation to alleviate cybersickness. Besides, it carefully examines SIto choose the path with smaller RW gains and restrict the quality degradation with IRS. On the contrary, the baselines ignore cybersickness and do not alleviate it by FoV shrinking and DoF simulation. In Fig. 4(c),IRWCA has better channel quality than the baselines because we find the proper timing for IRS adjustment to improve channel quality as the number of obstacles increases.

Fig. 4(d) and Fig. 4(e) investigate the impacts of MRC upper bound on the total cost and cybersickness. As the MRC upper bound increases, the system can choose edges with slightly larger RW gains. Unlike the baselines that prioritize shorter paths to reach the destination, IRWCA properly chooses the edges with better channel quality. IRWCA incurs the lowest total cost and cybersickness since it carefully evaluates CI and SI to reduce cybersickness with FoV shrinking and DoF simulation while maintaining channel quality with IRS.

Fig. 4(f), Fig. 4(g), and Fig. 4(h) explore the impact of VR adaptation (K). Users adapt to VR faster as K increases. The total MRC increases because the user can choose paths with larger RW gains without feeling dizzy. In contrast, baseline RP is designed for robots and its path planning strategy does not change based on the user immersion and cybersickness. In Fig. 4(f) and Fig. 4(g), IRWCA has the lowest total cost and cybersickness since it utilizes FoV shrinking and DoF simulation to alleviate cybersickness. In contrast to the baselines maximizing the channel quality, IRWCA examines CI to evaluate cybersickness. Moreover, it exploits SI to ensure the user's channel quality by adjusting IRS phase shift direction. In summary, IRWCA can effectively improve the user's signal strength and reduces the cybersickness by more than 50% compared to the baselines.

VI. Conclusion

In this paper, we exploit path planning with RW, IRS configuration, and cybersickness alleviation techniques to improve the VR experience for indoor VR applications. A new optimization problem PPCIC is formulated to minimize cybersickness accumulation and maintain the channel quality over time. To effectively solve PPCIC, we propose a novel algorithm IRWCA to select a path and its RW gains while adjusting FoV shrinking, DoF simulation, and IRS configuration by evaluating the CI and SI of each path segment. Simulation results demonstrate that IRWCA can improve more than 50% of SINR against the state-of-the-art algorithms for indoor IRS path planning systems. In the future, we will extend our system to handle multi-user scenarios with moving obstacles.

References

[1] C. Boletsis and J. E. Cedergren, "VR locomotion in the new era of virtual reality: an empirical comparison of prevalent techniques," *Advances in Human-Computer Interaction*, vol. 2019.

[2] H. Chen, S. Chen, and E. S. Rosenberg, "Redirected walking strategies in irregularly shaped and dynamic physical environments," in *IEEE VR*, 2018.

[3] N. C. Nilsson *et al.*, "15 years of research on redirected walking in immersive virtual environments," *IEEE Computer Graphics and Applications*, vol. 38, no. 2, pp. 44–56, 2018.

[4] F. Steinicke, G. Bruder *et al.*, "Estimation of detection thresholds for redirected walking techniques," *IEEE Trans Vis Comput Graph*, vol. 16, no. 1, pp. 17–27, 2009.

[5] T. Grechkin, J. Thomas *et al.*, "Revisiting detection thresholds for redirected walking: Combining translation and curvature gains," in *Proc. - SAP 2017 ACM Symp. Appl. Percept.*, 2016, pp. 113–120.

[6] P. Schmitz, J. Hildebrandt, and other, "You spin my head right round: Threshold of limited immersion for rotation gains in redirected walking," *IEEE Trans Vis Comput Graph*, vol. 24, no. 4, pp. 1623–1632, 2018.

[7] E. Langbehn, P. Lubos, G. Bruder, and F. Steinicke, "Bending the curve: Sensitivity to bending of curved paths and application in room-scale vr," *IEEE Trans Vis Comput Graph*, vol. 23, no. 4, pp. 1389–1398, 2017.

[8] T. Nescher, Y.-Y. Huang, and A. Kunz, "Planning redirection techniques for optimal free walking experience using model predictive control," in *2014 IEEE 3DUI*, pp. 111–118.

[9] Q. Wu and R. Zhang, "Towards smart and reconfigurable environment: Intelligent reflecting surface aided wireless network," *IEEE Communications Magazine*, vol. 58, no. 1, pp. 106–112, 2019.

[10] H. Alwazani *et al.*, "Intelligent reflecting surface-assisted multi-user miso communication: Channel estimation and beamforming design," *OJCOMS*, vol. 1, pp. 661–680, 2020.

[11] D. Zhang *et al.*, "Mobile user trajectory tracking for irs enabled wireless networks," *IEEE Transactions on Vehicular Technology*, 2021.

[12] X. Mu, Y. Liu, L. Guo, J. Lin, and R. Schober, "Intelligent reflecting surface enhanced indoor robot path planning: A radio map based approach," *IEEE Transactions on Wireless Communications*, 2021.

[13] N. Dużmańska, P. Strojny, and A. Strojny, "Can simulator sickness be avoided? a review on temporal aspects of simulator sickness," *Frontiers in psychology*, vol. 9, p. 2132, 2018.

[14] J. Hildebrandt, P. Schmitz *et al.*, "Get well soon! human factors' influence on cybersickness after redirected walking exposure in virtual reality," in *VAMR*. Springer, 2018, pp. 82–101.

[15] J. Kim and T. Park, "The onset threshold of cybersickness in constant and accelerating optical flow," *Applied Sciences*, vol. 10, no. 21, p. 7808, 2020.

[16] H. Kim *et al.*, "Clinical predictors of cybersickness in virtual reality (vr) among highly stressed people," *Scientific reports*, vol. 11, no. 1, pp. 1–11, 2021.

[17] A. S. Fernandes and S. K. Feiner, "Combating vr sickness through subtle dynamic field-of-view modification," in *2016 IEEE 3DUI*, pp. 201–210.

[18] S. Kim, S. Lee *et al.*, "An effective FoV restriction approach to mitigate VR sickness on mobile devices: An effective approach to mitigate VR sickness," *Journal of the Society for Information Display*, vol. 26, 2018.

[19] K. Carnegie and T. Rhee, "Reducing visual discomfort with hmds using dynamic depth of field," *IEEE computer graphics and applications*, vol. 35, no. 5, pp. 34–41, 2015.

[20] M. Weier, T. Roth, A. Hinkenjann, and P. Slusallek, "Foveated depth-of-field filtering in head-mounted displays," *ACM Transactions on Applied Perception*, vol. 15, no. 4, pp. 1–14, 2018.

[21] K.-Y. Liao, C.-W. Lin, D.-N. Yang, and W. Liao. (2021) Redirected walking with irs-assisted beamforming (full version). National Taiwan University, Tech. Rep. [Online]. Available: http://kiki.ee.ntu.edu.tw/~r08942125/RW.pdf

[22] E. Masehian and M. Amin-Naseri, "A voronoi diagram-visibility graph-potential field compound algorithm for robot path planning," *Journal of Robotic Systems*, vol. 21, no. 6, pp. 275–300, 2004.

[23] H.-P. Huang and S.-Y. Chung, "Dynamic visibility graph for path planning," in *2004 IEEE/RSJ IROS*, vol. 3, pp. 2813–2818.

[24] Q. Wu and R. Zhang, "Beamforming optimization for wireless network aided by intelligent reflecting surface with discrete phase shifts," *IEEE Transactions on Communications*, vol. 68, no. 3, pp. 1838–1851, 2019.

[25] M. Rietzler *et al.*, "Rethinking redirected walking: On the use of curvature gains beyond perceptual limitations and revisiting bending gains," in *2018 IEEE ISMAR*, pp. 115–122.

[26] J. Mayor, L. Raya *et al.*, "Multi-technique redirected walking method," *IEEE Transactions on Emerging Topics in Computing*, 2021.

[27] S. Abeywickrama, R. Zhang, Q. Wu, and C. Yuen, "Intelligent reflecting surface: Practical phase shift model and beamforming optimization," *IEEE Trans Commun*, vol. 68, no. 9, pp. 5849–5863, 2020.

[28] X. Ma *et al.*, "Intelligent reflecting surface enhanced indoor terahertz communication systems," *Nano Communication Networks*, vol. 24, p. 100284, 2020.

[29] Q. Wu and R. Zhang, "Intelligent reflecting surface enhanced wireless network via joint active and passive beamforming," *IEEE Transactions on Wireless Communications*, vol. 18, no. 11, pp. 5394–5409, 2019.

[30] C. You, B. Zheng, and R. Zhang, "Fast beam training for irs-assisted multiuser communications," *IEEE Wireless Communications Letters*, vol. 9, no. 11, pp. 1845–1849, 2020.

[31] Q. Wu and R. Zhang, "Intelligent reflecting surface enhanced wireless network: Joint active and passive beamforming design," in *2018 IEEE GLOBECOM*, pp. 1–6.

[32] N. L. Williams, A. Bera, and D. Manocha, "ARC: Alignment-based redirection controller for redirected walking in complex environments," *IEEE Trans Vis Comput Graph*, vol. 27, no. 5, pp. 2535–2544, 2021.

[33] M. Missura, D. D. Lee, and M. Bennewitz, "Minimal construct: Efficient shortest path finding for mobile robots in polygonal maps," in *2018 IEEE/RSJ IROS*, pp. 7918–7923.

[34] M. A. Zmuda, J. L. Wonser *et al.*, "Optimizing constrained-environment redirected walking instructions using search techniques," *IEEE Trans Vis Comput Graph*, vol. 19, no. 11, pp. 1872–1884, 2013.